RESEARCH PAPERS

Acta Cryst. (1994). B50, 511–518

Low-Temperature Structure of Lithium Nesosilicate, Li_4SiO_4, and its Li_{1s} and O_{1s} X-ray Photoelectron Spectrum

BY B. H. W. S. DE JONG AND D. ELLERBROEK

Institute for Earth Sciences and Vening Meinesz Institute for Geodynamic Research, Utrecht University, 3508TA Utrecht, The Netherlands

AND A. L. SPEK

Department of Chemistry and Bijvoet Center for Biomolecular Research, Utrecht University, 3508CH Utrecht, The Netherlands

(*Received* 13 *December* 1993; *accepted* 28 *February* 1994)

Abstract

Li_4SiO_4, $M_r = 119.84$, λ(Mo $K\alpha$) = 0.71073 Å, 150 K, monoclinic, $P2_1/m$, $a = 11.532$ (1), $b = 6.075$ (1), $c = 16.678$ (1) Å, $\beta = 99.04$ (1)°, $V = 1153.9$ (2) Å^3, μ(Mo $K\alpha$) = 5.3 cm^{-1}, $Z = 14$, $F(000) = 812$, $D_x = 2.414$ Mg m^{-3}, $R = 0.028$, $wR = 0.025$ for 2255 observed reflections with $I > 2.5\sigma(I)$. The crystal structure of lithium nesosilicate has been reinvestigated at 150 K and its room-temperature Li_{1s} and O_{1s} XPS spectrum has been measured. The principal difference with the previously reported structure [Tranqui, Shannon, Chen, Iijima & Baur (1979). *Acta Cryst.* B35, 2479–2487] is the introduction of a positional disorder model for two of the 19 Li positions. The Li_{1s} spectrum indicates the presence of an additional peak next to that observed for Li^{IV} in crystalline lithium phyllo- and inosilicates. This new peak indicative of Li^{V} is also observed during nucleation of glassy lithium disilicate. The O_{1s} spectrum of lithium nesosilicate indicates an XPS-derived charge of −0.77. The range of oxygen XPS-derived charges corresponds approximately one to one with that calculated using valence strength arguments.

Introduction

Adams (1993) observed during a Li_{1s} XPS study on internal nucleation of glassy lithium disilicate, $Li_2Si_2O_5$, a second peak which appeared after a 450°C heat treatment of the sample. The interpretation of this second peak has become an issue, as has its structural implication for the constitution of a nucleus formed in such glass. Li_{1s} XPS spectra of crystalline lithium phyllo- and inosilicates, with four-fold oxygen-coordinated lithium only, clearly indicated that this newly formed peak does not coincide in energy with Li^{IV}. Crystalline lithium nesosilicate has a larger variability in oxygen coordination around lithium than the lithium phyllo- and inosilicates, according to Tranqui, Shannon, Chen, Iijima & Baur (1979), Baur & Ohta (1982) and Völlenkle, Wittman & Nowotny (1968). It seemed, therefore, a good idea to test if the Li_{1s} XPS spectrum of this nesosilicate would show evidence for a site similar in XPS binding energy to that observed in nucleated glassy lithium disilicate. To clinch this issue unambiguously, it also seemed reasonable to reinvestigate the crystal structure of lithium orthosilicate as the previous determination by Tranqui, Shannon, Chen, Iijima & Baur (1979) has a relatively high R-factor, hence casting some uncertainty on the precise lithium positions and coordinations in particular. Our results indicate that the previously reported structure is essentially correct, apart from positional disorder for two Li atoms, and that the energy of the newly discovered Li_{1s} XPS peak in nucleated glassy lithium disilicate coincides with that for Li^{V} in nesosilicate.

Experimental

Crystals were synthesized by programmed cooling from an isochemical melt. As the melt temperature of the orthosilicate is 1528 K (Migge, 1988), the cooling trajectory was initiated with a 2 h hold at 1548 K followed by cooling to 1508 K with a ramp of 0.6 K min^{-1}. Optical inspection of the resulting large transparent and colorless crystals showed polysynthetic twinning for most crystals, as already observed by Tranqui, Shannon, Chen, Iijima & Baur (1979).

A specimen suitable for X-ray data collection was cut in protective mineral oil to the required shape and fixed on top of a Lindemann glass capillary with

Table 1. *Data collection and refinement parameters*

Crystal data	
Empirical formula	Li_4SiO_4
Formula weight	119.84
Crystal system	Monoclinic
Space group	$P2_1/m$*
a (Å)	11.532 (1)
b (Å)	6.075 (1)
c (Å)	16.678 (1)
β (°)	99.04 (1)
V (Å^3)	1153.9 (2)
Z	14
ρ_x (Mg m^{-3})	2.414
F(000)	812
μ(Mo $K\alpha$) (cm^{-1})	5.3
Crystal size (mm)	0.15 × 0.30 × 0.75
Data collection	
Temperature (K)	150
Radiation (Å)	Mo $K\alpha$ (monochromated) = 0.71073
θ_{min}, θ_{max} (°)	1.2, 27.5
Scan type	$\omega/2\theta$
Scan width $\Delta\omega$ (°)	0.80 + 0.35 tan θ
Reference reflections	−2 −2 −4, −2 2 −4, −5 2 −2 (no decay)
Data set hkl	−14:14; 0:7; −21:21
Total, unique data, R_{av}	5723, 2884, 0.020
Observed data $I > 2.5\sigma(I)$	2255
Refinement	
No. of parameters	262
R, wR, S	0.028, 0.025, 0.77
w^{-1}	$\sigma^2(F)$
$\Delta\rho$ range (e Å^{-3})	−0.37, 0.32
Mean and maximum shift/e.s.d.	0.003, 0.08

* See Baur & Ohta (1982).

vacuum grease. Data were collected on an Enraf–Nonius CAD-4T/rotating anode system at 150 K (60 kV, 150 mA). Accurate lattice parameters were derived from the SET4 setting angles (de Boer & Duisenberg, 1984) of 25 reflections in the range $9 < \theta < 16°$. The unit cell found by automatic reflection search and index procedures agrees well with the 'superlattice' cell reported by Tranqui, Shannon, Chen, Iijima & Baur (1979). 20 out of the 25 reflections found in the random search are only indexable in this 'superlattice'. The intensity data were corrected for Lp and absorption (*DIFABS*; Walker & Stuart, 1983; correction range 0.95: 1.09). The structure was refined on F by full-matrix least squares (*SHELX*76; Sheldrick, 1976) using the previously published coordinates (Tranqui, Shannon, Chen, Iijima & Baur 1979) as starting parameters. Two of the Li atoms were found to be disordered over two positions [Li(50)/Li(51) ~ 50:50; Li(65)/Li(60) ~ 50:50]. Their positions were refined with coupled occupation factors. Li atoms were refined with individual isotropic displacement parameters, all other atoms anisotropically. The empirical extinction parameter (Sheldrick, 1976) refined to 0.00191 (8). Neutral scattering factors were taken from Cromer & Mann (1968). Geometrical calculations and the *ORTEP* plot were performed using *PLATON* (Spek, 1990). Calculations were performed on a DEC5000 cluster. The data collection and refinement parameters are collected in Table 1.

Table 2. O_{1s} *and* Li_{1s} *XPS binding energies for lithium phyllo-, ino- and nesosilicate. The numbers in parentheses are the full width at half maximum values* (eV)

Compound	Li_{1s}	Li_{1s}	O_{1s}(br)	O_{1s}(nbr)
$Li_2Si_2O_5$	55.31 (1.75)		532.5 (1.8)	530.7 (1.7)
$Li_2Si_2O_3$	55.21 (1.75)		532.4 (1.9)	530.8 (1.9)
Li_4SiO_4	55.2 (2.0)	51.9 (2.0)		531.8 (2.4)

XPS spectra were collected on a Kratos XM-800 twin X-ray anode spectrometer using 400 W Mg $K\alpha_{1,2}$ radiation at a constant pass energy of 23.5 eV. The base pressure of the system during the experiment was better than 1×10^{-8} Torr. Signal resolution was optimized based on the full width at half maximum (FWHM) of the peak being less than 0.8 eV. The problem of charging effects due to the loss of photoelectrons was alleviated by using thin samples (10 × 10 × 1 mm) and by flooding the surface with an electron gun. Absolute peak position calibration was carried out by referencing to the $Auf_{7/2}$ photoelectron signal of a gold dot placed on the sample. Samples were slightly argon etched for a few minutes to remove surface contaminants. No changes were observed in the O_{1s} and Li_{1s} peak positions during sputtering.

Results

The O_{1s} and Li_{1s} XPS binding energies for lithium phyllo-, ino- and nesosilicate are collected in Table 2 and illustrated in Figs. 1 and 2. The atomic positions, equivalent displacement parameters U_{eq} and calculated valence strength V are collected in Table 3.* The crystal structure is shown in Fig. 3 and an *ORTEP* plot in Fig. 4. The relation of the present unit cell to the sevenfold smaller subcell reported by Völlenkle, Wittman & Nowotny (1968) is indicated by the broken lines.

Discussion

1. *Comparison with the lithium orthosilicate structure reported by Tranqui, Shannon, Chen, Iijima & Baur* (1979)

The structure determination of Tranqui, Shannon, Chen, Iijima & Baur (1979) has formed the basis for the structure refinement presented here. The

* A list of d(Li—Li) and Si—O—Li angles has been deposited with the IUCr (Reference: NA0052). Copies may be obtained through The Managing Editor, International Union of Crystallography, 5 Abbey Square, Chester CH1 2HU, England.

difference lies in the splitting up of the previously reported Li(51) and Li(65) site over two additional sites, Li(50) and Li(60), respectively; all four positions with an occupancy of 0.5. The Li(51)—Li(50) positions are 1.28 Å apart and the Li(65)–Li(60) positions 0.36 Å apart. Taking this disorder into account in the model significantly improved the weighted *R*-factor. It should be noted that the associated residual density for Li(50) was also observed by Tranqui, Shannon, Chen, Iijima & Baur (1979) but was considered to be an artifact. In hindsight, it can be understood why the displacement parameters of Li(51) and Li(65) in their refinement were found to be approximately twice as large as those for the other Li atoms.

Our refinement based on 2255 observed low-temperature data [*cf.* 1390 used by Tranqui, Shannon, Chen, Iijima & Baur (1979)] has no major effect on *d*(Si—O). The average values collected in Table 4 are similar to those found by Tranqui, Shannon, Chen, Iijima & Baur (1979), *viz.* 1.6363 (1.634), 1.6317 (1.628) and 1.6381 (1.641) Å. As might be anticipated, the refinement has a substantially larger effect on the observed *d*(Li—O).

A criterion to test the reliability of a structure is to calculate the valence strength to the O atom. We

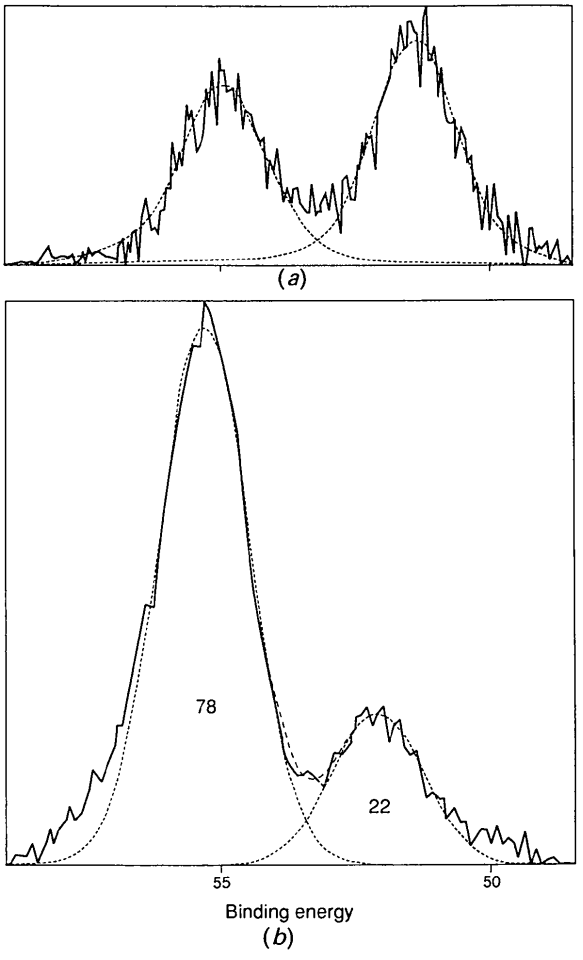

Fig. 1. Li_{1s} XPS spectra of lithium disilicate glass nucleated for 1 h at (*a*) 723 K and (*b*) crystalline lithium nesosilicate. The peak with the largest binding energy corresponds to Li^{IV}, as observed in the lithium meta- and phyllosilicates, and the peak with the smallest binding energy to $Li^{V/VI}$. The total area fitted by the two Gaussians is 94.5%.

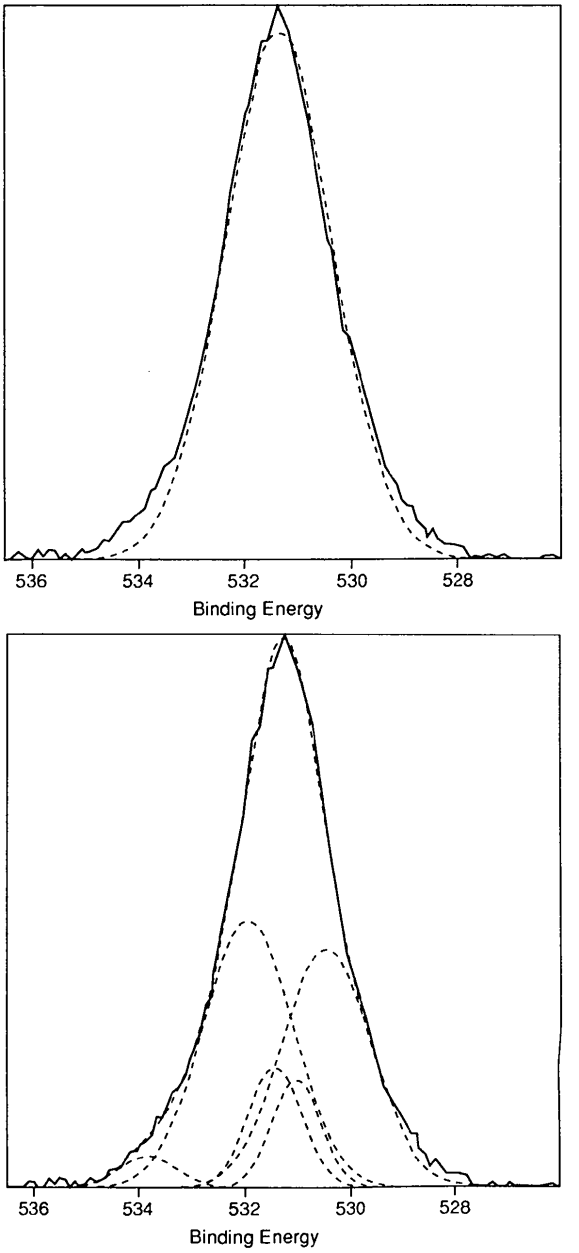

Fig. 2. O_{1s} XPS spectra of lithium nesosilicate. 94.9% of the area can be fitted with a single Gaussian. With five Gaussians, 98.7% of the total area under the peak can be fitted.

Table 3. *Positional parameters, equivalent isotropic displacement parameters U_{eq} and valence V for lithium orthosilicate*

$$U_{eq} = (1/3)\Sigma_i\Sigma_j U_{ij} a_i^* a_j^* \mathbf{a}_i.\mathbf{a}_j.$$

Li_4SiO_4	x	y	z	U_{eq} (Å^2)	V (CN#)*
Si(11)	0.34163 (6)	1/4	0.00662 (4)	0.0039 (2)	−3.89 (IV)
Si(12)	0.75400 (6)	1/4	0.13848 (5)	0.0043 (2)	−3.87 (IV)
Si(13)	0.52292 (6)	3/4	0.28628 (4)	0.0036 (2)	−3.86 (IV)
Si(14)	0.20097 (6)	1/4	0.29134 (4)	0.0037 (2)	−3.89 (IV)
Si(15)	0.04009 (6)	1/4	0.57822 (4)	0.0039 (2)	−3.91 (IV)
Si(16)	0.10533 (6)	3/4	0.14378 (5)	0.0042 (2)	−3.86 (IV)
Si(17)	0.61539 (6)	1/4	0.42877 (4)	0.0035 (2)	−3.87 (IV)
O(11)	0.35828 (9)	0.0270 (3)	0.06061 (7)	0.0053 (4)	2.03 (V)
O(21)	0.20147 (14)	1/4	−0.03832 (11)	0.0065 (6)	1.91 (VI)
O(31)	0.42052 (15)	1/4	−0.06607 (11)	0.0052 (6)	2.08 (V)
O(12)	0.78618 (9)	0.0323 (3)	0.19691 (7)	0.0071 (4)	1.91 (VI)
O(22)	0.61856 (14)	1/4	0.09887 (10)	0.0053 (6)	2.00 (IV)
O(32)	0.84629 (15)	1/4	0.07235 (11)	0.0058 (6)	1.99 (VI)
O(13)	0.50229 (9)	0.5292 (3)	0.23058 (7)	0.0052 (4)	2.03 (V)
O(23)	0.66579 (15)	3/4	0.32421 (11)	0.0061 (6)	1.95 (VII)
O(33)	0.44438 (15)	3/4	0.35907 (11)	0.0054 (6)	1.99 (V)
O(14)	0.21590 (9)	0.0269 (3)	0.34544 (7)	0.0055 (4)	2.02 (V)
O(24)	0.06236 (15)	1/4	0.24352 (11)	0.0070 (6)	1.93 (VI)
O(34)	0.28297 (15)	1/4	0.22079 (11)	0.0057 (6)	2.08 (V)
O(15)	0.06893 (10)	0.0321 (3)	0.63729 (7)	0.0060 (4)	1.89 (VI)
O(25)	−0.09109 (14)	1/4	0.52927 (11)	0.0059 (6)	1.95 (IV)
O(35)	0.13291 (15)	1/4	0.51416 (10)	0.0058 (6)	1.97 (VI)
O(16)	0.07437 (10)	0.5328 (3)	0.08453 (7)	0.0072 (4)	1.89 (VI)
O(26)	0.23875 (15)	3/4	0.18764 (11)	0.0055 (6)	2.00 (IV)
O(36)	0.01023 (14)	3/4	0.20779 (11)	0.0058 (6)	2.03 (VI)
O(17)	0.65440 (9)	0.0288 (3)	0.48129 (7)	0.0051 (4)	2.04 (V)
O(27)	0.47630 (14)	1/4	0.39500 (10)	0.0060 (6)	1.97 (IV)
O(37)	0.69526 (15)	1/4	0.35310 (11)	0.0060 (6)	1.95 (VI)
Li(12)	0.3838 (2)	0.0038 (6)	0.40796 (17)	0.0072 (6)	−1.08 (IV)
Li(15)	0.1878 (2)	0.5033 (6)	0.45404 (17)	0.0078 (6)	−1.10 (IV)
Li(16)	0.3374 (2)	0.5082 (7)	0.17286 (17)	0.0076 (6)	−1.13 (IV)
Li(17)	0.5237 (2)	0.4943 (7)	0.11688 (17)	0.0077 (6)	−1.10 (IV)
Li(21)	0.7282 (4)	3/4	0.1400 (3)	0.0124 (10)	−0.96 (IV)
Li(23)	0.4175 (4)	1/4	0.5489 (3)	0.0163 (11)	−0.87 (IV)
Li(24)	0.1350 (4)	1/4	0.1435 (3)	0.0123 (11)	−0.92 (IV)
Li(25)	0.0279 (4)	3/4	0.5702 (3)	0.0128 (11)	−0.86 (IV)
Li(32)	0.4529 (4)	1/4	0.2763 (3)	0.0095 (9)	−0.98 (IV)
Li(36)	0.2710 (4)	3/4	0.3038 (3)	0.0098 (10)	−1.02 (IV)
Li(37)	0.4108 (4)	3/4	0.0173 (3)	0.0088 (10)	−1.06 (IV)
Li(41)	0.1918 (3)	0.5308 (7)	0.01313 (18)	0.0117 (7)	−1.08 (IV)
Li(43)	0.6657 (2)	0.0340 (6)	0.26721 (17)	0.0090 (6)	−1.09 (IV)
Li(46)	0.0503 (3)	0.5299 (7)	0.29348 (18)	0.0120 (7)	−1.09 (IV)
Li(51)†	0.9478 (6)	0.4564 (15)	0.1553 (5)	0.014 (2)	−0.91 (V)
Li(53)	0.2382 (3)	0.0391 (6)	0.59744 (17)	0.0105 (6)	−1.00 (V)
Li(61)	0.8588 (4)	3/4	0.2667 (3)	0.0141 (11)	−0.84 (VI)
Li(64)	0.0037 (5)	1/4	0.0123 (3)	0.0186 (12)	−0.75 (VI)
Li(65)†	0.8556 (10)	1/4	0.2978 (7)	0.010 (3)	−0.77 (VI)
Li(50)†	0.0887 (6)	0.0460 (14)	−0.1241 (4)	0.011 (2)	−0.90 (V)
Li(60)†	0.8809 (11)	1/4	0.2875 (8)	0.015 (3)	−0.77 (VI)

* The bond-valence parameters are 1.624 and 1.466 for Si—O and Li—O bonds, respectively, according to Brese & O'Keeffe (1991). The coordination number is given in parentheses in latin numerals behind the calculated valence.

† Occupancy 0.5.

have calculated this for lithium orthosilicate using the parametrization of Brese & O'Keeffe (1991). Our results show that the electrostatic valence strength for oxygen varies between 1.89 and 2.08 in this structure, indicating a well balanced charge distribution. Of course, such parametrization can also be used to test how well the electron-donating atoms, Li and Si, are balanced. These results are also collected with a negative sign in Table 3, indicating the loss of electrons or a decrease in valence strength of these atoms. The calculated values for silicon clusters vary in a very narrow range between −3.86 and −3.91. For lithium, the range is much broader, varying between −0.75 and −1.13 to an extent reflecting a more dubious oxygen coordination criterion around this atom.

Inspection of *d*(Li—O) in Table 4 indicates that 13 of the 20 Li atoms occur in regular tetrahedra with values ranging between 1.863 (3) and 2.144 (5) Å. These two extrema contribute 0.3419 and 0.1596, respectively, in valence strength to oxygen. The

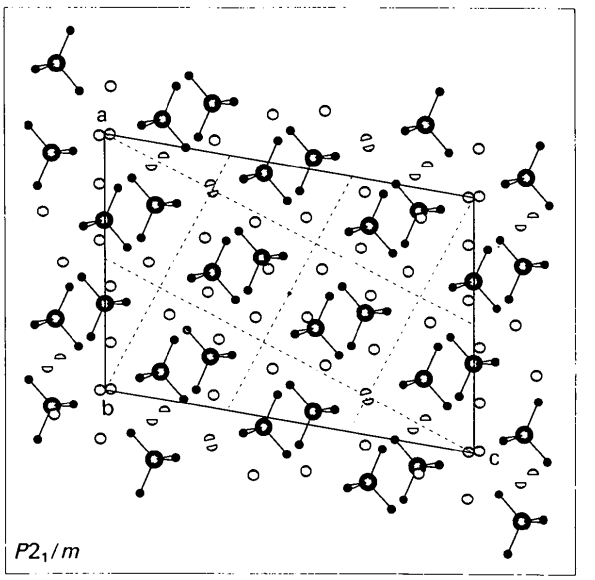

Fig. 3. Projection of the structure of Li_4SiO_4 down the *b*-axis. The seven times smaller subcell (Völlenkle, Wittman & Nowotny, 1968) is indicated. The partial occupancy of Li 50/51 and Li 60/65 is indicated by half spheres.

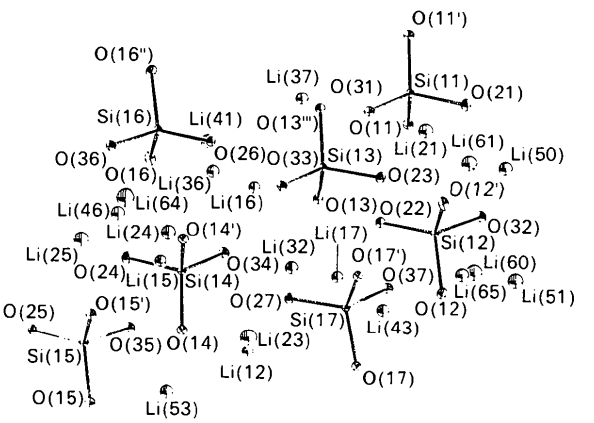

Fig. 4. *ORTEP* (see experimental: *PLATON*) plot drawn at the 60% probability level for Li_4SiO_4. The indicated symmetry symbols are: (i) x, $1/2 - y$, z; (ii) x, $3/2 - y$, z.

Table 4. *Bond distances* (Å) *and angles in* Li_4SiO_4

Silicon coordination					
Si(11)—O(11) × 2	1.6211 (17)	Si(11)—O(21)	1.6715 (18)	Si(11)—O(31)	1.6257 (19)
Si(12)—O(12) × 2	1.6499 (17)	Si(12)—O(22)	1.5975 (18)	Si(12)—O(32)	1.6483 (19)
Si(13)—O(13) × 2	1.6275 (17)	Si(13)—O(23)	1.6696 (19)	Si(13)—O(33)	1.6243 (19)
Si(14)—O(14) × 2	1.6221 (17)	Si(14)—O(24)	1.6705 (19)	Si(14)—O(34)	1.6209 (19)
Si(15)—O(15) × 2	1.6522 (17)	Si(15)—O(25)	1.6022 (18)	Si(15)—O(35)	1.6265 (18)
Si(16)—O(16) × 2	1.6533 (17)	Si(16)—O(26)	1.6965 (18)	Si(16)—O(36)	1.6460 (19)
Si(17)—O(17) × 2	1.6282 (17)	Si(17)—O(27)	1.6144 (18)	Si(17)—O(37)	1.6748 (19)
Average	1.6363 (17)		1.6317 (18)		1.6381 (19)
Lithium coordination					
Li(12)—O(27)	1.869 (3)	Li(15)—O(14^{iii})	1.898 (3)	Li(16)—O(26)	1.898 (4)
Li(12)—O(33^{i})	1.926 (3)	Li(15)—O(25^{iv})	1.924 (3)	Li(16)—O(34)	1.911 (4)
Li(12)—O(17^{ii})	1.975 (3)	Li(15)—O(17^{v})	1.970 (3)	Li(16)—O(11^{iii})	1.937 (3)
Li(12)—O(14)	2.055 (3)	Li(15)—O(35)	1.993 (3)	Li(16)—O(13)	1.996 (3)
Li(17)—O(22)	1.895 (4)	Li(21)—O(31^{vi})	1.949 (5)	Li(23)—O(17^{v})	1.918 (3)
Li(17)—O(31^{vi})	1.928 (4)	Li(21)—O(21^{vi})	1.991 (5)	Li(23)—O(17^{ii})	1.918 (3)
Li(17)—O(13)	1.962 (3)	Li(21)—O(12^{iii})	2.022 (3)	Li(23)—O(33^{viii})	2.031 (5)
Li(17)—O(11^{iii})	1.993 (3)	Li(21)—O(12^{vii})	2.022 (3)	Li(23)—O(23^{viii})	2.457 (5)
Li(24)—O(34)	1.970 (5)	Li(25)—O(25^{iv})	1.914 (5)	Li(32)—O(27)	1.956 (5)
Li(24)—O(24)	1.981 (5)	Li(25)—O(15^{iii})	2.061 (3)	Li(32)—O(13)	1.980 (3)
Li(24)—O(16^{iii})	2.047 (3)	Li(25)—O(15^{vii})	2.061 (3)	Li(32)—O(13^{iii})	1.980 (3)
Li(24)—O(16)	2.047 (3)	Li(25)—O(35^{iv})	2.144 (5)	Li(32)—O(34)	2.032 (5)
Li(36)—O(26)	1.914 (5)	Li(37)—O(22^{vi})	1.924 (5)	Li(41)—O(21)	1.921 (4)
Li(36)—O(14^{iii})	1.963 (3)	Li(37)—O(11^{vii})	1.964 (3)	Li(41)—O(16)	1.939 (4)
Li(36)—O(14^{vii})	1.963 (3)	Li(37)—O(11^{iii})	1.964 (3)	Li(41)—O(32^{vi})	1.950 (4)
Li(36)—O(33)	2.066 (5)	Li(37)—O(31^{vi})	1.987 (5)	Li(41)—O(11^{iii})	1.990 (4)
Li(43)—O(13^{iii})	1.926 (3)	Li(46)—O(24)	1.908 (4)	Li(50)—O(36^{x})	2.070 (8)
Li(43)—O(37)	1.933 (3)	Li(46)—O(15^{iv})	1.929 (4)	Li(50)—O(12^{xi})	2.082 (7)
Li(43)—O(12)	1.954 (3)	Li(46)—O(36)	1.959 (4)	Li(50)—O(32^{xii})	2.083 (8)
Li(43)—O(23^{i})	1.970 (4)	Li(46)—O(14^{iii})	1.999 (4)	Li(50)—O(16^{x})	2.090 (7)
				Li(50)—O(21)	2.165 (7)
Li(53)—O(17^{ii})	1.985 (3)	Li(61)—O(36^{xiii})	2.134 (5)	Li(64)—O(16^{x})	2.169 (4)
Li(53)—O(23^{viii})	2.030 (4)	Li(61)—O(15^{v})	2.143 (4)	Li(64)—O(16^{xv})	2.169 (4)
Li(53)—O(37^{viii})	2.038 (4)	Li(61)—O(15^{xiv})	2.143 (4)	Li(64)—O(16^{iii})	2.181 (4)
Li(53)—O(35)	2.125 (4)	Li(61)—O(12^{vii})	2.166 (3)	Li(64)—O(16)	2.181 (4)
Li(53)—O(15)	2.159 (3)	Li(61)—O(12^{iii})	2.166 (3)	Li(64)—O(32^{xvi})	2.207 (6)
		Li(61)—O(23)	2.558 (5)*	Li(64)—O(21)	2.553 (6)*
Li(65)—O(15^{ii})	2.138 (7)	Li(51)—O(36^{xiii})	2.066 (9)	Li(60)—O(15^{v})	2.149 (8)
Li(65)—O(15^{v})	2.138 (7)	Li(51)—O(16^{xiii})	2.069 (8)	Li(60)—O(15^{ii})	2.149 (8)
Li(65)—O(12^{iii})	2.190 (9)	Li(51)—O(32)	2.085 (8)	Li(60)—O(12^{iii})	2.169 (11)
Li(65)—O(12)	2.190 (9)	Li(51)—O(12^{iii})	2.090 (7)	Li(60)—O(12)	2.169 (11)
Li(65)—O(37)	2.192 (12)	Li(51)—O(24^{xiii})	2.207 (8)	Li(60)—O(24^{xiii})	2.323 (13)
Li(65)—O(24^{xiii})	2.680 (12)*			Li(60)—O(37)	2.552 (13)
Oxygen coordination					
O(11)—Si(11)	1.6213 (17)	O(12)—Si(12)	1.6501 (17)	O(13)—Si(13)	1.6277 (17)
O(11)—Li(16^{iii})	1.937 (3)	O(12)—Li(43)	1.954 (3)	O(13)—Li(43^{iii})	1.926 (3)
O(11)—Li(37^{i})	1.964 (3)	O(12)—Li(21^{xvii})	2.022 (3)	O(13)—Li(17)	1.962 (3)
O(11)—Li(41^{iii})	1.990 (4)	O(12)—Li(50^{xi})	2.082 (7)†	O(13)—Li(32)	1.980 (3)
O(11)—Li(17^{iii})	1.993 (3)	O(12)—Li(51^{iii})	2.090 (7)†	O(13)—Li(16)	1.996 (3)
		O(12)—Li(61^{i})	2.166 (3)		
		O(12)—Li(60)	2.169 (11)†		
		O(12)—Li(65)	2.190 (9)†		
O(14)—Si(14)	1.6223 (17)	O(15)—Si(15)	1.6524 (17)	O(16)—Si(16)	1.6535 (17)
O(14)—Li(15^{iii})	1.898 (3)	O(15)—Li(46^{xviii})	1.929 (4)	O(16)—Li(41)	1.939 (4)
O(14)—Li(36^{i})	1.963 (3)	O(15)—Li(25^{i})	2.061 (3)	O(16)—Li(24)	2.047 (3)
O(14)—Li(46^{iii})	1.999 (4)	O(15)—Li(65^{vii})	2.138 (7)†	O(16)—Li(51^{xvi})	2.069 (8)†
O(14)—Li(12)	2.055 (3)	O(15)—Li(61^{vii})	2.143 (4)	O(16)—Li(50^{ix})	2.090 (7)†
		O(15)—Li(60^{viii})	2.149 (8)†	O(16)—Li(64^{ix})	2.169 (4)
		O(15)—Li(53)	2.159 (3)	O(16)—Li(64)	2.181 (4)
O(17)—Si(17)	1.6284 (17)	O(21)—Si(11)	1.6714 (18)	O(22)—Si(12)	1.5974 (18)
O(17)—Li(23^{viii})	1.918 (3)	O(21)—Li(41^{iii})	1.921 (4)	O(22)—Li(17^{iii})	1.895 (4)
O(17)—Li(15^{viii})	1.970 (3)	O(21)—Li(41)	1.921 (4)	O(22)—Li(17)	1.895 (4)
O(17)—Li(12^{ii})	1.975 (3)	O(21)—Li(21^{xii})	1.991 (5)	O(22)—Li(37^{xii})	1.914 (5)
O(17)—Li(53^{ii})	1.985 (3)	O(21)—Li(50^{iii})	2.165 (7)†		
		O(21)—Li(50)	2.165 (7)†		
		O(21)—Li(64)	2.553 (6)*		
O(23)—Si(13)	1.6695 (19)	O(24)—Si(14)	1.6705 (19)	O(25)—Si(15)	1.6021 (18)
O(23)—Li(43^{iii})	1.970 (4)	O(24)—Li(46^{iii})	1.908 (4)	O(25)—Li(25^{xviii})	1.914 (5)
O(23)—Li(43^{vii})	1.970 (4)	O(24)—Li(46)	1.908 (4)	O(25)—Li(15^{xx})	1.914 (3)
O(23)—Li(53^{xiv})	2.030 (4)	O(24)—Li(24)	1.981 (5)	O(25)—Li(15^{xviii})	1.914 (3)
O(23)—Li(53^{v})	2.030 (4)	O(24)—Li(51^{xix})	2.207 (8)†		
O(23)—Li(23^{v})	2.458 (5)	O(24)—Li(51^{xvi})	2.207 (8)†		
O(23)—Li(61)	2.558 (5)*	O(24)—Li(60^{xvi})	2.324 (13)†		

Table 4 (*cont.*)

O(26)—Si(16)	1.5965 (18)	O(27)—Si(17)	1.6143 (18)	O(31)—Si(11)	1.6260 (19)
O(26)—Li(16)	1.898 (4)	O(27)—Li(12^{iii})	1.869 (3)	O(31)—Li(17^{xv})	1.928 (4)
O(26)—Li(16^{xxi})	1.898 (4)	O(27)—Li(12)	1.869 (3)	O(31)—Li(17^{xxii})	1.928 (4)
O(26)—Li(36)	1.914 (5)	O(27)—Li(32)	1.956 (5)	O(31)—Li(21^{xv})	1.949 (5)
		O(27)—Li(23)	2.755 (5)†	O(31)—Li(37^{xv})	1.987 (5)
O(32)—Si(12)	1.649 (2)	O(33)—Si(13)	1.6247 (19)	O(34)—Si(14)	1.6212 (19)
O(32)—Li(41^{xxii})	1.950 (4)	O(33)—Li(12^{iii})	1.926 (3)	O(34)—Li(16^{iii})	1.911 (4)
O(32)—Li(41^{xxiii})	1.950 (4)	O(33)—Li(12^{vii})	1.926 (3)	O(34)—Li(16)	1.911 (4)
O(32)—Li(50^{vi})	2.083 (8)†	O(33)—Li(23^{v})	2.031 (5)	O(34)—Li(24)	1.970 (5)
O(32)—Li(50^{xi})	2.083 (8)†	O(33)—Li(36)	2.066 (5)	O(34)—Li(32)	2.032 (5)
O(32)—Li(51^{iii})	2.085 (8)†				
O(32)—Li(51)	2.085 (8)†				
O(32)—Li(64^{xiii})	2.207 (6)				
O(35)—Si(15)	1.6268 (19)	O(36)—Si(16)	1.6463 (19)	O(37)—Si(17)	1.6752 (19)
O(35)—Li(15^{iii})	1.993 (3)	O(36)—Li(46^{xxi})	1.959 (4)	O(37)—Li(43^{iii})	1.933 (3)
O(35)—Li(15)	1.993 (3)	O(36)—Li(46)	1.959 (4)	O(37)—Li(43)	1.933 (3)
O(35)—Li(53^{iii})	2.125 (3)	O(36)—Li(51^{xxiii})	2.066 (9)†	O(37)—Li(53^{ii})	2.038 (4)
O(35)—Li(53)	2.125 (3)	O(36)—Li(51^{xvi})	2.066 (9)†	O(37)—Li(53^{v})	2.038 (4)
O(35)—Li(25^{xviii})	2.144 (5)	O(36)—Li(50^{ix})	2.070 (8)†	O(37)—Li(65)	2.192 (12)†
		O(36)—Li(50^{xv})	2.070 (8)†	O(37)—Li(60)	2.553 (13)†
		O(36)—Li(61^{xvi})	2.134 (5)		

Angles

⟨O—Si(11)—O⟩	109.34 (7)	⟨Si—O—Li⟩	110.69 (8)
⟨O—Si(12)—O⟩	109.4 (7)	range:	80.81 (15)–175.9 (4)
⟨O—Si(13)—O⟩	109.39 (7)		
⟨O—Si(14)—O⟩	109.35 (7)		
⟨O—Si(15)—O⟩	109.42 (7)		
⟨O—Si(16)—O⟩	109.38 (7)		
⟨O—Si(17)—O⟩	109.42 (7)		
range			
105.27 (6)–114.53 (10)			

* Within the oxygen coordination sphere around Li(61) occur two Li atoms at 2.560 (5) Å; in the oxygen coordination sphere around Li(64) and Li(65) one Li atom occurs at 2.457 (7) and 2.392 (13) Å, respectively.

† The Li(50), Li(51), Li(60) and Li(65) positions are only half filled, thus the formal coordination to these sites has to be counted as a half. The cut-off value used has been 2.6 Å for the coordination sphere around Li and 2.8 Å for the coordination sphere around O.

Symmetry codes: (i) $x, -1+y, z$; (ii) $1-x, -y, 1-z$; (iii) $x, 1/2-y, z$; (iv) $x, 1/2+y, 1-z$; (v) $1-x, 1/2+y, 1-z$; (vi) $1-x, 1/2+y, -z$; (vii) $x, 1+y, z$; (viii) $1-x, -1/2+y, 1-z$; (ix) $-x, 1/2+y, -z$; (x) $-x, -1/2+y, -z$; (xi) $1-x, -y, -z$; (xii) $1-x, -1/2+y, -z$; (xiii) $1+x, y, z$; (xiv) $1-x, 1-y, 1-z$; (xv) $-x, 1-y, -z$; (xvi) $-1+x, y, z$; (xvii) $1+x, 3/2-y, z$; (xviii) $-x, -1/2+y, 1-z$; (xix) $-1+x, 1/2-y, z$; (xx) $-x, 1-y, 1-z$; (xxi) $x, 3/2-y, z$; (xxii) $1-x, 1-y, -z$; (xxiii) $-1+x, 3/2-y, z$; (xxiv) $1+x, 1/2-y, z$.

coordination around Li(23) becomes more questionable. Here, the case can be made for a threefold coordinated Li atom as one d(Li—O) is 2.457 Å, contributing only 0.07 valence units to oxygen. No clear cut criterion exists as to decide whether this O atom should still be included in the lithium coordination sphere, in particular considering the occurrence of d(Li—Li), which are substantially shorter than 2.457 Å [⟨d(Li—Li)⟩ = 2.496 (5) Å; range 2.385 (4)–2.595 (6) Å].

There are three regular fivefold oxygen-coordinated Li atoms in this structure, Li(50), Li(51) and Li(53), with d(Li—O) varying between 1.984 (3) and 2.207 (8) Å, contributing 0.2453 and 0.1361 valence units, respectively, to the O atom. More ambiguous are the four sixfold oxygen-coordinated lithium sites, Li(60), Li(61), Li(64) and Li(65). All these sites contain one d(Li—O) outlier, which, if included, again results in including Li atoms which are closer in distance than this outlying O atom to the central Li atom. Their valence strength contributions vary between 0.0784 and 0.0524. The calculated valence strengths to lithium for sixfold coordinated sites show the largest deviations from the −1 value for ideal lithium, even though all outlier d(Li—O) values from Table 4 are included in its value.

Although we have considered in our electrostatic valence strength calculations for Li atoms all d(Li—O) collected in Table 4, it may be more reasonable to take as a criterion that only Li—O distances are considered which fall inside the smallest d(Li—Li) observed range. The consequence of this would be that any d(Li—O) beyond 2.384 (4) Å, the minimum d(Li—Li), would not be included in the oxygen coordination sphere around lithium. Thus, only one three-, 13 four- and seven fivefold oxygen-coordinated Li atoms would be present and no sixfold coordinated atoms.

The coordination around oxygen varies between 4 and 7, as shown in Table 4. Again outliers occur at large coordination number. For instance, O(23) has a

fairly tight clustering of d(O—Li) values, except for the two values at 2.457 (5) and 2.558 (5) Å, contributing 0.1030 and 0.0797 valence units to this O atom. These two Li atoms account for 10% of the total valence strength received by this atom. Still, within the coordination sphere calculated within a cut-off value of 2.60 Å around each O atom, only Li atoms but no other atoms occur.

Two angular variations are of interest in this crystal, the O—Si—O and Si—O—Li angles. Selected values for these two angles are collected in Table 4. Perusal of the O—Si—O angles in this Table indicates that the local tetrahedral environment around Si is, as anticipated, fairly close to symmetric. A much larger scatter occurs in the Si—O—Li angles varying between 175.9 and 83.8°.

2. Li_{1s} *and* O_{1s} *XPS spectra*

The reason for carrying out this research is illustrated in Fig. 1. The top diagram is taken from the thesis of Adams (1993) and illustrates her discovery concerning the occurrence of a second peak in the Li_{1s} spectrum of an internally nucleated lithium disilicate glass. The bottom diagram shows the Li_{1s} spectrum of lithium orthosilicate, showing two peaks comparable in energy to those observed for nucleated glass. The peak with the largest binding energy can be identified with Li^{IV}, as inspection of Table 2 indicates. The peak with the smallest binding energy and lower intensity is due to Li^{V}. The intensity ratios between the two peaks are in the ballpark for those measured in lithium nesosilicate. Clearly, the lithium site generated during nucleation in lithium disilicate is similar to Li^{V}. The implications of this lithium coordination for the structure of nuclei in this system will be reported elsewhere (Adams & de Jong, 1994).

The average valence strength donated by Li^{IV} is -1.024 and for $Li^{V/VI}$ -0.86. Li^{IV} has, therefore, a more positive charge than $Li^{V/VI}$. The relation between formal charge and Li_{1s} XPS binding energy (BE) is then given by the following formula

$$Li_{1s}BE\ (eV) = 20.12\ (Q_{Li}) + 34.597.$$

It should be noted that Q_{Li} is a formal charge rather than a quantum mechanically derived one.

A more fundamental relation between charge and XPS shifts is available for oxygen. Utilizing the *ab initio* Hartree–Fock results for this atom and taking care of its chemical environment by construction of a Watson sphere results in the following formula (Bagus & Bauschlicher, 1982; Adams & de Jong, 1993; de Jong, 1989)

$$Q_O = -4.372 + [385.023 - 8.976(545.509 - O_{1s}BE)]^{1/2}/4.488.$$

The average oxygen charge, Q_O, calculated in this manner for lithium orthosilicate, -0.77 esu, is comparable to that calculated for oxygen in the $H_6Si_2O_7$ molecule using a Mulliken analysis of *ab initio* Hartree–Fock, or semi-empirical CNDO/2, calculated results (Burkhard, de Jong, Meyer & van Lenthe, 1991; de Jong & Brown, 1980; Passier, 1993).

The FWHM of the O_{1s} spectrum is 2.5 eV, ranging from 533 to 530.5 eV. The calculated oxygen charges at these two values are -0.69 and -0.85 eV, respectively, *i.e.* a range of 0.16 electrostatic charge units. It is of interest to note that the calculated valence strength range for the 21 O atoms in the lithium nesosilicate is 0.19 units, according to Table 3. Thus, there is a close and gratifying correspondence between the range of XPS-derived oxygen charges and those associated with parametrized valence strength calculations according to Brese & O'Keeffe (1991).

Summary and concluding remarks

The crystal structure of lithium nesosilicate has been refined and its O_{1s} and Li_{1s} photoelectron spectrum measured. The oxygen coordination around lithium is four- or fivefold. These two coordinations cause a shift in the Li_{1s} photoelectron spectrum of 3.4 eV. The XPS-derived oxygen charge and that based on valence-strength calculations show a close, within experimental error, one-to-one correspondence. It seems, therefore, that this parametrization is a good measure to evaluate molecular dynamical results of alkali silicate glasses, providing a classical analogue to electron-density functional methods.

The crystallographic work (ALS) was supported by the Netherlands foundation for Chemical Research (SON) with financial aid from the Netherlands Organization for Scientific Research (NWO). XPS spectra were collected at the Center for Ceramic Research at Rutgers University, Piscataway, NJ. We are indebted to Dr Adams and Dr Hensley for these spectra.

References

ADAMS, J. W. (1993). *Morphogenesis in Lithium Disilicate Glass: Internal Nucleation in Amorphous Structures*, 170 pp. Thesis, Cambridge Univ., England.

ADAMS, J. W. & DE JONG, B. H. W. S. (1993). Terra nova 5, Abstract Supplement 1, p. 484.

ADAMS, J. W. & DE JONG, B. H. W. S. (1994). MRS 1993 Fall Meeting Symp. Proc., Vol. E. MRS Mat. Res. Soc., Pittsburgh, Pensylvania, USA. In preparation.

BAGUS, P. S. & BAUSCHLICHER, C. W. (1982). *J. Electron Spectrosc. Relat. Phenom.* **20**, 183–190.

BAUR, W. H. & OHTA, T. (1982). *J. Solid State Chem.* **44**, 50–53.

BOER, J. L. DE & DUISENBERG, A. J. M. (1984). *Acta Cryst.* A**40**, C410.

BRESE, N. E. & O'KEEFFE, M. (1991). *Acta Cryst.* B47, 192–197.
BURKHARD, D. J. M., DE JONG, B. H. W. S., MEYER, A. J. H. M. & VAN LENTHE, J. H. (1991). *Geochim. Cosmochim. Acta*, **55**, 3453–3458.
CROMER, D. T. & MANN, J. B. (1968). *Acta Cryst.* A24, 321–324.
JONG, B. H. W. S. DE (1989). *Glass: Ullmann's Encycl. Ind. Chem. A*, **12**, 365–432.
JONG, B. H. W. S. DE & BROWN, G. E. (1980). *Geochim. Cosmochim. Acta*, **44**, 491–511.
MIGGE, H. (1988). *J. Nucl. Mat.* **151**, 101–107.
PASSIER, H. F. (1993). *Ab Initio Molecular Orbital Calculations on Silicate Systems*, 45 pp. Drs Thesis, Utrecht University.
SHELDRICK, G. M. (1976). *SHELX76. Program for Crystal Structure Determination*. Univ. of Cambridge, England.
SPEK, A. L. (1990). *Acta Cryst.* A46, C34.
TRANQUI, D., SHANNON, R. D., CHEN, H. Y., IIJIMA, S. & BAUR, W. H. (1979). *Acta Cryst.* B35, 2479–2487.
VÖLLENKLE, H., WITTMAN, A. & NOWOTNY, H. (1968). *Monatsh. Chem.* **99**, 1360–1371.
WALKER, N. & STUART, D. (1983). *Acta Cryst.* A39, 158–166.

Acta Cryst. (1994). B50, 518–524

Mechanism of Crystal Dendrite Formation in KNO_3

BY L. J. SOLTZBERG, STELLA A. FAPPIANO, LESLEE D. GRIFFITH, LORI E. HIDEK, SHARON A. OFEK AND LUCCI L. SUAREZ

Department of Chemistry, Simmons College, 300 The Fenway, Boston, MA 02115, USA

(*Received* 12 *July* 1993; *accepted* 21 *January* 1994)

Abstract

KNO_3 dendrites grown from thin layers of supersaturated aqueous solution display dendrite branches growing along the ⟨031⟩, ⟨041⟩ and ⟨051⟩ crystallographic directions. These directions do not correspond to faces in normal polyhedral crystals of KNO_3 and, thus, are directions of fast growth in normal crystals. As the growth rate of a normal KNO_3 crystal is increased by cooling the solution, a sharp transition occurs from growth in the [010] direction to growth in one or more of these ⟨0k1⟩ directions. Interference photomicrographs show that this transition is accompanied by a distortion of the concentration field around the crystal, which further accelerates growth along ⟨0k1⟩. We suggest that these two effects constitute a positive-feedback mechanism responsible for dendrite self-organization.

Introduction

Pattern-formation in nature has long been a subject of contemplation (Thompson, 1961). Extensive study of nonlinear dynamics during the past two decades has led to an understanding of pattern formation in a wide variety of systems (see, for example, Nicolis & Prigogine, 1977; Field & Burger, 1985; Thompson & Stewart, 1986). Diverse studies have shown that systems governed by nonlinear dynamical equations are subject to bifurcations in time and/or space as the systems are driven away from equilibrium. Temporal bifurcations lead to oscillatory behavior and spatial bifurcations lead to symmetry-reducing pattern formation; these phenomena are referred to collectively as 'self-organization'.

Perhaps no other inanimate object so embodies the fascination of pattern formation as does a snowflake. The classic lacy snowflake is a dendritic crystal. Dendrite formation has, therefore, been a subject of scrutiny from the perspective of nonlinear dynamics; practical applications of understanding and controlling dendrite formation have also motivated such work (Langer, 1989, 1992). The dynamical approach focuses on the differential equations describing the continuous variables which govern the behavior of a system. For dendrites growing either from the melt or from solution, the principal factors have been taken to be diffusion of either heat or mass, respectively, and surface tension (Ben-Jacob, Goldenfeld, Langer & Schön, 1983). This continuum thermodynamic viewpoint is specifically and intentionally different from a molecular mechanistic perspective (Langer, 1980), although recent theoretical studies have included kinetic anisotropy at the growing crystal surface (Classen, Misbah, Müller-Krumbhaar & Saito, 1991).

Other investigators have sought an understanding of dendrites in the molecular mechanism of crystal growth. Sunagawa (1981, 1987) has summarized earlier work suggesting that the transition from normal to dendritic habit is related to growth mechanism. The key to this change has been taken to be the 'roughening transition' in which growing surfaces of the crystal are converted from smooth to rough by changes in either temperature or supersaturation (Bennema & van der Eerden, 1987).